Development of sandwich test coupons with continuous protective layers for accurate determination of the tensile failure strain of unidirectional carbon fibre reinforced composites

Czél G.

Composites: Part A 187 (2024) 108440

Contents lists available at ScienceDirect

Composites Part A

journal homepage: www.elsevier.com/locate/compositesa

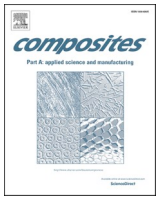

Development of sandwich test coupons with continuous protective layers for accurate determination of the tensile failure strain of unidirectional carbon fibre reinforced composites

Gergely Czél

Department of Polymer Engineering, Faculty of Mechanical Engineering, Budapest University of Technology and Economics, Műegyetem rkp. 3, H-1111 Budapest, Hungary
MTA-BME Lendület Sustainable Polymers Research Group, Műegyetem rkp. 3, H-1111 Budapest, Hungary

ARTICLE INFO

Keywords:
A. Carbon fibre
A. Glass fibre
D. Mechanical testing
Specimen

ABSTRACT

Recently introduced unidirectional (UD) carbon fibre reinforced epoxy (CF/EP) tensile test coupons with continuous protective layers were developed further by comparing three coupon designs with different layer integration techniques. Consistent experimental data was generated with high sample number and low scatter. Thermal residual strains were considered in case of two coupon designs where the layers were integrated at elevated temperature. A curve-fitting-based strength evaluation method is proposed for the sandwich coupons since this parameter cannot be evaluated directly. The sandwich type coupons yielded statistically significant increase in their average failure strain compared to that of the baseline tabbed coupons. In contrast, the three sandwich coupon types did not show significant differences. Therefore, the sandwich coupon type made by bonding cured UD composite layers together at room temperature is proposed for further application as they allow for full delamination at CF/EP layer fracture and do not require thermal strain correction during the evaluation.

1. Introduction

Carbon fibre reinforced composites are increasingly preferred for high-performance applications where high stiffness and strength paired with low density are of key importance. Since the architecture of composite materials is more complicated than that of traditional homogeneous structural materials, numerical modelling is an essential design tool which can provide useful results only if appropriate input is fed into the model. Therefore, accurate determination of the basic mechanical properties, incl. elastic modulus, failure strain and strength of unidirectional (UD) carbon fibre reinforced epoxy (CF/EP) is crucial. However, tabbed prismatic test coupons recommended by standard test methods ASTM D3039/D3039M [1] and ISO 527–5 [2] tend to fail prematurely at the gripped sections due to stress concentrations. One traditional approach to solve this problem is to taper the end-tabs by machining as recommended by the standards or to produce a thicker gripped section by adding extra plies into the laminate in the gripped sections [3,4]. The tapered end-tabs are prone to de-bonding in the section not forced to the coupon by the grips and did not increase the strength in some cases [5,6,7], while the intrinsically tapered coupons are more effective but complicated to fabricate. Another approach to reducing the stress concentrations is to widen the coupons towards the gripped sections, which was investigated by using new test coupon geometries like the butterfly and long butterfly [8,9]. These coupon types can reduce stress concentrations but seem to be prone to premature splitting in the widening section, and the fabrication of the shaped coupons requires significant extra effort. Czél et al. investigated UD interlayer hybrid composites under tensile loading extensively as part of a group at the University of Bristol with the scope of generating pseudo-ductility by fragmentation of a thin high-strength CF/EP layer between thicker glass fibre/epoxy (GF/EP) layers [10,11]. Inspired by some of the failed attempts, when the hybrid laminates delaminated upon CF/EP layer failure, Czél et al. proposed co-cured interlayer hybrid tensile test coupons (see Fig. 1. b) for eliminating the stress concentrations [12] and reported consistent gauge-section CF/EP layer fractures with high failure strains near that of the failure strain of the fibres quoted by their manufacturer. A 2D finite element analysis was presented to explain the protective role of continuous UD GF/EP layers co-cured together with the CF/EP plies. Kumar et al. [9] at DTU combined the butterfly shape with continuous protective layers. They obtained significantly (up to 16 %) higher strength of their 2 mm thick high-strength CF/EP coupons compared to those of

E-mail address: czel@pt.bme.hu.

https://doi.org/10.1016/j.compositesa.2024.108440
Received 2 April 2024; Received in revised form 27 August 2024; Accepted 29 August 2024
Available online 30 August 2024

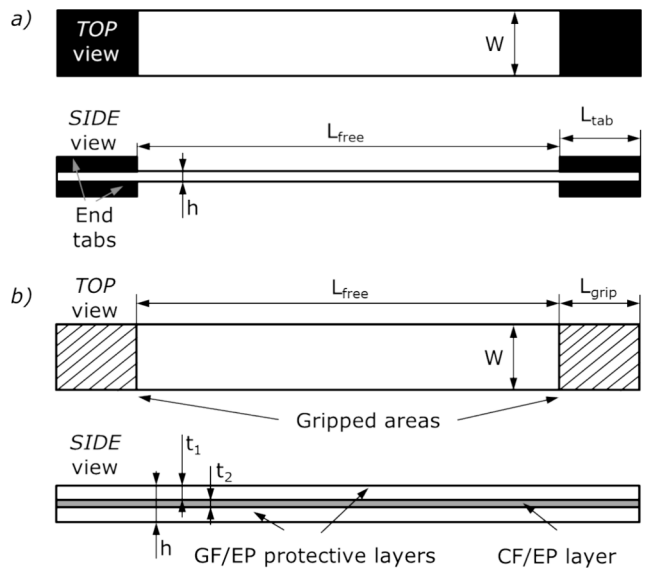

Fig. 1. Schematics of a) standard coupon with end-tabs, b) sandwich coupon with continuous protective layers.

the standard baseline ones. The protective layers were bonded to the CF/EP plates. A number of further studies were published, where the authors simulated the gripped region of tensile test coupons and their surroundings numerically to analyse the stress concentrations and came up with favourable designs [6,7,13,14]. The numerical modelling efforts and coupon type evolution are well summarised in a recent paper by Fazlali et al. [15]. The group at KU Leuven proposed a new coupon type with arrow-shaped tabs and compared the performance of five different coupon designs of the most promising ones, incl. rectangular and tapered tabbed, co-cured continuously protected and butterfly-shaped ones for quasi-static tension [15] and tension–tension fatigue [16] loading. They also presented a thorough 3D finite element analysis, which confirmed that the continuous protecting layers fully eliminate the stress concentrations. The continuously protected high modulus CF/EP coupons showed 7.5 % higher average failure strain than the standard tabbed ones. It was also highlighted that the arrow-shaped end-tabs performed almost as good as the continuous protective layers in quasi-static tension by smearing out the stress concentration over a larger area and reducing the width direction stresses coming from different Poisson's ratios and constrained coupon ends.

Since the novel coupon design with continuous protective layers was applied successfully recently by a few groups (mainly using a co-cured, layered structure), an experimental campaign was initiated to develop them further by exploring and improving the available layer integration techniques. It was also noted that the experimental data found in the literature was generated with a wide range of CF with different properties, and the increment between the failure strains obtained with standard and novel specimen designs was also various. These findings indicate that a focussed experimental study comparing different continuously protected specimen designs could be of interest. The new type sandwich coupons presented in this paper were designed with standardisation in mind and therefore kept as simple and reproducible as possible. A key feature of the presented experimental study is that three sandwich coupon designs are directly compared, with focus on the layer integration method, using the same constituent materials.

2. Design

This section provides information about the concept, the laminate design and the materials utilised during the development of the new type tensile test coupons. The presented coupon designs are called "sandwich" type to indicate that some of them cannot be interpreted as a hybrid composite any more like the co-cured one presented first in the literature [12].

2.1. Concept

The motivation for developing new type tensile test coupons for UD carbon fibre reinforced composites was to improve the accuracy of failure strain and strength determination of these high-performance materials extensively applied in safety–critical applications. As it was reported in the literature, e.g. by Fazlali et al. [15] and experienced by the author, current standard coupons (Fig. 1.a) suffer from premature failure caused by stress concentrations at the edges of the end-tabs due to changes in the cross-section. Therefore, modelling and design efforts may be based on inaccurate key mechanical property values.

The author proposed hybrid composite coupons with continuous UD GF/EP protective layers (Fig. 1.b) to address this issue and showed promising results in [12] with four thin plies of TR30 CF/EP (total thickness: 0.12 mm) co-cured with standard thickness S-glass/epoxy plies. Fig. 2 shows the schematic stress–strain response of the coupons with continuous protective layers with a significant load drop marking the fracture of the CF/EP layer. However, the structure of the hybrid laminates and its effect on the test results was not investigated in detail. The author as well as Fazlali et al identified the variable thickness and transverse undulation of the CF/EP layer on cross-section optical micrographs [15]. The uneven nature of the CF/EP layer may affect its connection to the protecting GF/EP layers through interlocking due to nesting effects and bias the tensile test results. Another drawback of the otherwise simple and effective co-curing approach (see section 3.2.1 for details) is the presence of thermal residual strain between the CF/EP and the GF/EP layers due to their different coefficients of thermal expansion (CTE) and the elevated layer integration temperature. This effect can be compensated for, but obtaining accurate CTE values for both UD composite layers is usually challenging.

This rigorous experimental study aims at systematically comparing all the feasible layer integration approaches with pre-impregnated composite sheets (prepregs) and a conventional tabbed coupon type as a baseline if they show any difference in the measured failure strain and strength of the UD CF/EP material. After careful assessment of the practical aspects of manufacturing three-layer plates from CF/EP and GF/EP prepreg plies, the following layer integration approaches were selected for investigation:

- **Co-curing:**
  This is the simplest approach when all the prepreg plies necessary to build the three-layer sandwich structure with the desired layer thicknesses are laid-up and cured in an autoclave in one operation.
- **Curing-on:**
  It is possible to lay-up and cure the CF/EP plate separately in an autoclave and then lay-up the necessary number of GF/EP prepreg

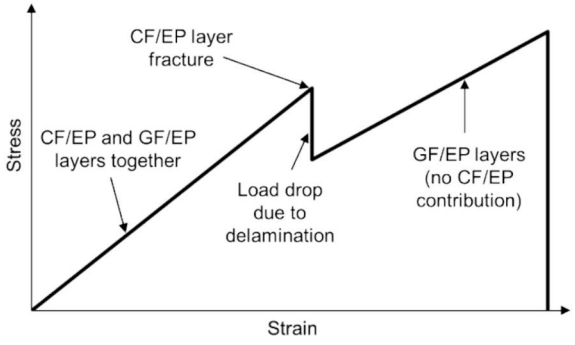

Fig. 2. Schematic showing the typical stress–strain response of tensile test coupons with continuous protective layers.

plies onto the cured plate and cure them in the autoclave in a second cycle.

- **Bonding:**
  The CF/EP and two GF/EP plates of the designed thicknesses can be cured separately. The three plates can then be bonded at room temperature to make a sandwich plate with continuous UD GF/EP protective layers on the CF/EP layer. Room temperature bonding eliminates the thermal residual strains and allows a more accurate evaluation of the test results by removing a possible source of uncertainty.

Table 1 summarises the key practical aspects of the sandwich coupon designs. The geometry of the investigated sandwich coupons (see Fig. 1b) was kept as close as possible to those of standard ones for direct comparability (i.e. same volume and dimensions). Therefore, the same nominal cross-sectional geometry as the typical values in the standards was used: width $w = 15$ mm, CF/EP layer thickness $t_2 = 1$ mm and free length $L_{free} = 150$ mm with nominal gripped/tabbed length being ~ 50 mm at both ends. Table 2 summarises the standard and selected coupon geometries.

2.2. Materials

The materials considered for design and used for the experiments were CF/EP and S-glass/epoxy (GF/EP) prepregs from Hexcel made with IM7 intermediate modulus (IM) carbon (Hexcel) and Flite Strand S-glass (Owens Corning) fibres. Both prepregs had the aerospace grade 913 epoxy resin (Hexcel) for full compatibility. Araldite 2011 (Huntsman) two-part epoxy adhesive was used to bond the end-tabs and the GF/EP and CF/EP plates for specific coupon types at room temperature. Basic properties of the applied fibres and prepreg systems can be found in Tables 3 and 4.

2.3. Unidirectional sandwich laminate design

As discussed in section 2.1, the CF/EP layer thickness was kept at $t_2 = 1$ mm for consistency with current material testing standards. For simplicity, as a first attempt, the thicknesses of the GF/EP protective layers were also set to $t_1 = 1$ mm, resulting in a 3 mm thick sandwich laminate construction with a simple UD lay-up sequence: [SG_4/$IM7_4$/SG_4] where SG stands for UD S-GF/EP and IM7 stands for UD CF/EP prepreg plies.

Design criteria for UD interlayer hybrid composites were identified earlier [12] to ensure stable pseudo-ductile failure. Since the structure of the proposed sandwich coupons is analogous, these criteria were adopted directly for design in this study. However, in this specific case, fragmentation of the CF/EP layer (which would not be feasible anyway due to the way too high energy release rate of the thick layer) is not desired. Instead, immediate delamination of the layers at the first CF/EP layer fracture was ensured. Inequality (1) highlights that the energy release rate (G_{II}) of the sandwich laminate at the fracture strain of the CF/EP layer (ε_{2b}) must be higher than the estimated mode II fracture toughness (G_{IIC}) of the laminate to achieve this.

$$G_{II} = \frac{\varepsilon_{2b}^2 E_2 t_2 (2E_1 t_1 + E_2 t_2)}{8E_1 t_1} > G_{IIC} \tag{1}$$

Table 1
Comparison of the different sandwich coupon designs.

Sandwich coupon type	Manufacturing steps (excluding coupon cutting)	Shape of CF/EP layer	Thermal residual strains
Co-cured	1	undulated	yes
Cured-on	2	flat	yes
Bonded	2	flat	no

Table 2
Nominal geometry of the standard and sandwich coupons.

	Width [mm]	Overall length [mm]	Free length [mm]	Tab/protection thickness [mm]
ASTM D3039	15	250	138	1.5
ISO 527–5	15	250	150	0.5–2
Sandwich coupons	15	250	150	1

Where: E_1 is the elastic modulus of the GF/EP layers in the loading direction, E_2 is the elastic modulus of the CF/EP layer in the loading direction, t_1 is the thickness of one GF/EP layer, t_2 is the thickness of the CF/EP layer as shown in Fig. 1.

A G_{IIC}=2.0 N/mm, which was obtained with similar materials and *co-cured* sandwich construction, but with thinner layers in [17] is considered as an estimated baseline. The same G_{IIC} value was considered as a conservative estimation for the bonded layer interfaces as well. Substituting the material and geometric parameters in equation (1) yields a G_{II}=21.7 N/mm at the expected failure strain of the CF/EP layer, which is significantly higher than the estimated G_{IIC} of 2.0 N/mm therefore, immediate delamination is expected, so the proposed construction is suitable.

Another important design criterion is to make sure that the GF/EP layers do not fail together with the CF/EP layer, i.e. they can take the full load of the sandwich coupon without the contribution of the CF/EP layer. This is preferred in order to keep the sandwich coupon in one piece after CF/EP fracture until it is unloaded to allow failure location assessment. Equation (2) assuming a fracture in the CF/EP layer, but no delamination was presented in [18] to determine the minimum thickness of the GF/EP layers required for them to survive the first CF/EP fracture. Coupon design for immediate delamination at CF/EP fracture makes this criterion conservative because, in displacement control, a significant load drop takes place when the CF/EP layer fractures in the coupon. This large and sudden load drop immediately reduces and spreads the stress in the glass layers, making them less critical than suggested by equation (2).

$$t_1 > \frac{\varepsilon_{2b} E_2 t_2}{2E_1(\varepsilon_{1b} - \varepsilon_{2b})} \tag{2}$$

Where (ε_{1b}) is the expected failure strain of the GF/EP layers.

After substituting to equation (2), the minimum thickness for one GF/EP layer is $t_{1min} = 1.0$ mm, which is considered suitable based on the conservative nature of the design criterion.

Please note that an important goal of the design process is to keep the thickness of the GF/EP protective layers as low as possible to reduce the maximum load during the tensile test. This is important because wedge action grips generate a clamping force proportional to the main tensile load and may damage the fully UD sandwich coupons, which are sensitive to transverse compression. In order to maintain a simple geometry which is still safe enough against premature GF/EP failure, the initial 1 mm layer thickness was kept for both CF/EP and GF/EP layers. Table 5 shows the selected configuration and the results of the design calculations.

3. Experimental

The manufacturing processes of the different type coupons, the methods and equipment applied for mechanical testing are presented in this section.

3.1. Coupon geometry

The coupons tested within the study were 15 mm wide prismatic tensile test coupons (see Fig. 1 and Table 1). The baseline coupons were

Table 3
Properties of the applied fibres based on manufacturer's datasheet values.

Fibre type	Manufacturer	Diameter [μm]	Elastic modulus [GPa]	Strain to failure [%]	Tensile strength [GPa]	Density [kg/m^3]	CTE[a] [1/K]
Flite Strand S-glass	Owens Corning	9	92	3.6–4.4	3.3–4.1	2450	$3.4{\cdot}10^{-6}$
IM7 carbon	Hexcel	5.2	276	1.9	5.7	1780	$-6.4{\cdot}10^{-7}$

[a] Coefficient of thermal expansion

Table 4
Cured ply properties of the applied UD composite prepregs.

Material designation	Manufacturer	Nominal fibre areal density[a] [g/m^2]	Fibre volume fraction[a] [%]	Nominal cured ply thickness[b] [mm]	Elastic modulus[b] [GPa]	Failure strain [%]
S-glass/913 epoxy	Hexcel	305	49	0.25	47.1	3.9[c]
IM7 carbon/913 epoxy	Hexcel	220	50	0.25	139.3	1.6[d]

[a] Based on the manufacturer's data.
[b] Estimated using manufacturer's data.
[c] Conservative average experimental value obtained with similar material for design purpose.
[d] Manufacturer's data for 60% fibre volume fraction

Table 5
Sandwich laminate design selected for testing. (Key: *SG* −S-glass fibre, *CF* −carbon fibre, subscripts indicating the number of plies in a block).

Sandwich configuration [Lay-up sequence]	Fibre areal densities of the constituent plies [g/m^2]	Nominal thickness h [mm]	Calculated G_{II} at CF/EP nominal failure strain (1.6 %) [N/mm]	Minimum thickness of GF/EP protective layers [mm]	Predicted elastic modulus [GPa]
$[SG_4/CF_4/SG_4]$	$[305_4/220_4/305_4]$	[1/1/1]	21.7	1.0	77.5

made of 1 mm thick IM7/913 CF/EP plates with 1.5 mm thick woven GF/EP end-tabs, and the sandwich coupons were made of the same CF/EP material with two full-length 1 mm thick protective layers integrated to the test plate with the methods listed in section 2.1. The nominal free and overall length of the coupons were L_{free} = 150 mm and 250 mm, respectively.

3.2. Coupon manufacturing

As mentioned in section 2.1. a key aspect of this study is the comparison of the selected layer integration methods and the results obtained with the different sandwich- and the standard baseline coupons. Therefore, a detailed description of the manufacturing techniques is provided for the four different coupon types as significant know-how is lying especially in the bonding procedure.

3.2.1. Baseline tabbed coupons

Operation 1: Lay-up and autoclave curing

Baseline coupons were made by manually stacking four 300x300 mm plies of IM7/913 prepreg with the same orientation, placing them on a flat Al tool plate and curing them in an autoclave (Olmar ATV 1100/2000) for 60 min at 125 °C and 7 bar pressure (recommended by the manufacturer). The prepreg stacks were fully wrapped in release film, and sufficiently thick silicone strips were placed around them to stop resin bleed-out from the plies. 20 mm thick Al top plates were used to make sure that the thickness variation of the cured plates is minimised. The same procedure and cure conditions were used for all coupon types and prepreg materials as the matrix was the same 913 epoxy in them.

Operation 2: End-tabbing and coupon cutting

Please find details of the standard procedure of end-tabbing in the Appendix (section 6.1). Individual coupons were cut out from the tabbed test plate with a Mutronic Diadisc 5200 type precision cutter using a diamond wheel. The same equipment was used to cut all type coupons.

3.2.2. Co-cured sandwich coupons

Operation 1: Lay-up and autoclave curing

Co-cured sandwich coupons were made by manually stacking 12 plies to have a UD $[SG_4/IM7_4/SG_4]$ plate and autoclave-curing it. For full details, please see the Appendix (section 6.2.).

Operation 2: Coupon cutting with a diamond wheel

Notes: In case of all type sandwich coupons, no composite end-tabs were bonded. The continuous UD GF/EP protective layers were able to avoid premature failure due to damage from the sharp nails of the grips, if P80 grade sandpaper tabs were applied to the coupons (see Fig. 3). The process of making the co-cured sandwich coupons was found simpler than that for the baseline type mainly due to the absence of end-tabbing. However, additional cost of the GF/EP protective material must be considered.

3.2.3. Cured-on sandwich coupons

Operation 1: Lay-up and autoclave curing of the CF/EP plate

In the first step, the IM7/913 CF/EP plate is laid-up and cured the same way as the baseline test plate.

Operation 2: Lay-up and autoclave curing the GF/EP layers onto the cured CF/EP plate

In this second step, two blocks of four S-glass/epoxy plies were laid-up manually and debulked under vacuum before they were stacked together in the same orientation with the cured and degreased CF/EP plate. The UD sandwich stack was then debulked together for min. 10 min to ensure strong initial adhesion between the layers. The sandwich plate was finally cured in the autoclave.

Operation 3: Coupon cutting with a diamond wheel

3.2.4. Bonded sandwich coupons

Operation 1: Lay-up and autoclave curing of individual CF/EP and GF/EP plates

For this coupon type, the three constituent plates are cured separately in an autoclave, the same way as the baseline test plate. It is useful to cure all three plates on one tool plate at the same time to minimise the possible effects of slightly different curing conditions.

Operation 2: Bonding of the three plates

In this step, the task is to bond three 1x300x300 mm UD plates at room temperature with minimum tolerance in the orientation of the layers and the uniform thickness of the adhesive layer, preferably without expensive equipment. After a few trials with conventional techniques suitable for bonding smaller areas, it was realised that it is a major challenge to

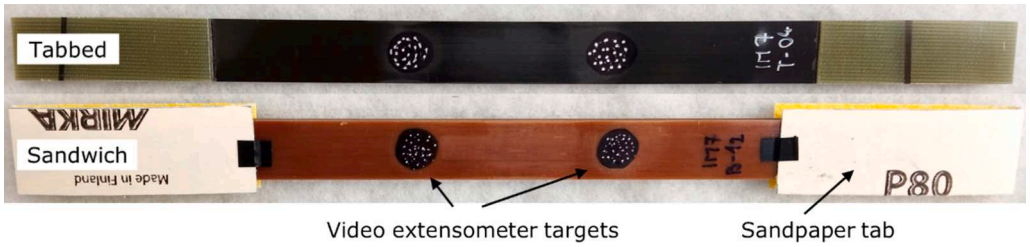

Fig. 3. Baseline tabbed and sandwich coupon prepared for tensile testing.

execute the bonding of the 300x300 mm areas without any blisters or macroscopic air bubbles and with precise positioning of the three plates. Therefore, full details of the systematically developed bonding procedure are included in the Appendix (section 6.3.).

Operation 3: Coupon cutting with a diamond wheel

3.3. Mechanical test procedure

Testing of the new type and baseline standard coupons was executed under uniaxial quasi-static tensile loading and displacement control at a crosshead speed of 5 mm/min (total test time 100–200 s) on a computer-controlled Zwick Z250 type 250 kN rated universal electro-mechanic test machine fitted with a regularly calibrated 250 kN load cell and 100 kN rated Instron 2716–003 type manual wedge action grips. The strains were measured optically on one side of the coupons, with a Mercury Monet type video-extensometer using two 5 MPixel resolution cameras to cancel the possible effect of out-of-plane displacements of the coupons. An approx. 50 mm gauge length and white dots (made with sharp tip paint marker) on a black background (made with blunt tip permanent marker) were used for high contrast to make targets for the video-extensometer (see Fig. 3). Four out of ten coupons of each series were fitted with HBM K-LA11K6/350LE strain gauges (6 mm active grid length, 350 Ω resistance), two of them had strain gauges on both sides for validation purpose. A Spider 8–30 type data acquisition unit was used to record the strain data. Data acquisition frequency was consistently set to 10 Hz for the test machine, the video-extensometer and the electronic strain gauge system. The ends of the coupons were protected using P80 grit sandpaper tabs secured with small pieces of insulating tape. The length of the tabs was designed to hang 5 mm over the serrated part of the grips. After a separate study of different grit-size sandpapers (P40-P100), P80 grit size was found optimal, therefore it was adapted for the experiments. A minimum of ten coupons were tested for each coupon type. The failure strain and stress of the sandwich coupons were determined at the last data point before the major stress drop due to CF/EP layer fracture (see Fig. 2). The rest of the stress–strain curves was truncated for simplicity. The elastic moduli of the individual coupons were determined by fitting lines manually to the initial part of their stress–strain curves in the strain regime 0–0.3 %. Fig. 3. shows photographs of a baseline tabbed and a sandwich coupon prepared for tensile testing.

3.4. Optical microscopy

Cross sections of the sandwich coupons were investigated with a Keyence VHX-5000 type digital microscope equipped with a VH-Z20UT Zoom Lens (20x-200x range). The samples were prepared by embedding them in epoxy resin and polishing them on a Buehler Beta type machine with 320 (P400) grit sandpaper, 9 and 3 μm MataDi Supreme polycrystalline diamond, and 0.05 μm MasterPrep Alumina suspensions, all supplied by Buehler.

4. Results and discussion

The results of the experimental campaign are presented and discussed in this section.

4.1. Structure of the sandwich coupons

Fig. 4 shows the structure of the sandwich coupons with their CF/EP and GF/EP layers integrated in different ways. Obvious transverse (width direction) undulation can be observed in case of directly *co-curing* all the prepreg plies in one step due to the non-uniform tow distributions in the plies (see Fig. 4a). The uneven interfaces may result in unnecessarily good connection between the tested and the protective layers due to potential mechanical interlocking, which is hard to predict and control, therefore this structure was found undesirable. The *cured-on* version has a completely flat CF/EP layer (see Fig. 4b) since it was made separately, and the protective layers were laid-up and cured onto the solid CF/EP plate. This is preferable from a mechanical point of view as the layers can separate easier upon CF/EP layer fracture.

The *bonded* sandwich coupon has completely flat composite layers (made separately) connected by uniform thickness adhesive layers. A few air bubbles are visible within the adhesive layers (see Fig. 4c), but they do not form large blisters, which could compromise the load transfer between the layers in the gripped region. The thickness of the adhesive layers was measured at 5 points along the coupon width and recorded as 291.2 ± 5.9 μm and 295.5 ± 4.6 μm, which is rather thick, but it was not found detrimental to the test results. The role of the adhesive layer is to transfer the tensile load from the grips and the protective layers to the CF/EP layer in the sandwich coupon through shear, so no interlaminar shear through the adhesive layer in the gauge section was expected as the tensile strain across the sandwich coupon thickness is considered uniform. Since the length of the gripped section (50 mm) was sufficiently long, the shear strength of the adhesive was not a critical design factor. Sufficient but not too strong adhesion was considered ideal to ensure "easy" delamination of the layers at CF/EP layer fracture, eliminating any influence of the protective layers on the failure strain of the examined central layer.

4.2. Tensile test results

The strains measured with the two different methods (video vs strain

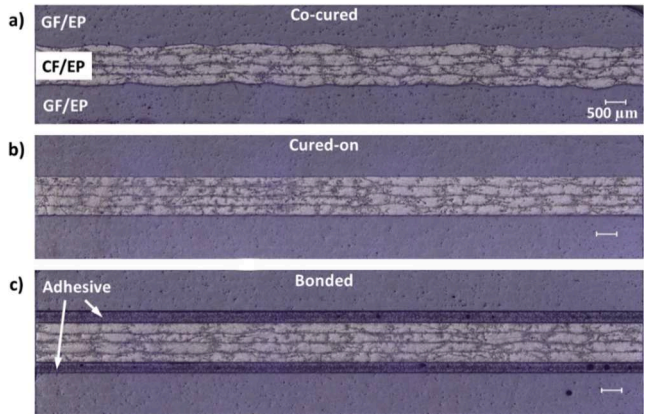

Fig. 4. Cross-sectional optical micrographs of three different type sandwich coupons.

gauge) were carefully compared, and a decision to use the video extensometer data for the presentation of the results was made as only small relative differences were recorded (less than 1 rel.% in 11/17 cases, less than 1.5 rel.% in 5/17 cases). Fig. 5a shows the stress–strain curves of the *baseline tabbed* coupon series with a second-order polynomial (green dashed line) fitted to all the individual curves with regression.

The test graphs were consistent with limited scatter and showed visible non-linearity, as expected based on previous observations by the author and other researchers. The role of the pure CF/EP coupon series was to provide a baseline for comparison of the failure strains obtained with the novel sandwich coupons and enable the failure stress estimation of the sandwich coupons, where direct determination of the stress in the CF/EP layer is not possible. The type of the function fitted to the stress–strain curves was selected by assuming a linear change of the elastic modulus with strain as proposed by Kumar et al. [9]. This approach yields a second-order polynomial for the stress–strain relation. The parameters of the fitted function are summarised in equation (3).

$$\sigma = 114.2\varepsilon^2 + 1390.9\varepsilon - 2.930 \tag{3}$$

Good fit of the function (green dashed line on Fig. 5a) to the test curves was confirmed visually and indicated by the high $R^2 = 0.998$. The small negative constant term is considered negligible (less than 0.2 %) to the average stress at failure. Strengths of the CF/EP layer in sandwich coupons can be estimated by extrapolating the fitted polynomial until the failure strain of the CF/EP (marked with a major stress drop as shown in Fig. 6a) in the selected coupon. Fig. 5b shows the failed *baseline* coupons and confirms that failure near the edges of the end-tabs was dominant, as expected for this series.

Fig. 6a shows a typical full stress–strain curve of a sandwich coupon, including the major stress drop at the failure strain of the CF/EP layer. The aggregated stress–strain curves of the *co-cured* sandwich coupon series are presented in Fig. 6b after evaluating the stresses using the full thickness of the sandwich coupons (please note the reduction in stresses compared to the baseline series). The aggregated curves of the test series were truncated at the failure strain of the CF/EP layer for clarity. The test curves were consistent with limited scatter, and the non-linearity was reduced as expected, as the UD GF/EP protective layers were reported to show a linearly elastic tensile response. Fig. 6c shows the appearance of the test coupons after CF/EP layer fracture and the failure locations based on visual observations. It is worth highlighting that the layers of the coupons remained bonded in the gripped areas, therefore handling and failure location determination was convenient, and all coupons failed within the gauge section.

The *cured-on* sandwich coupon series produced very consistent stress–strain curves with little scatter, especially in the failure strain (see Fig. 7a). Very similar results were obtained with these and the co-cured coupons. The failure locations were also found in the gauge section for all coupons (see Fig. 7b).

Fig. 8a shows the stress–strain response of the *bonded* sandwich coupon series. The scatter of the data is also small in this case, but the stresses are reduced in general by the increased thickness of the coupons due to the thick bond lines. Only one CF/EP fracture was observed at the edge of the gripped section of the coupon (see Fig. 8b). A significant amount of the adhesive was falling out of the sandwich coupons as small plates, possibly due to the dynamic effects of the CF/EP fracture and sudden delamination.

4.3. Consideration of thermal residual strains

As mentioned earlier, the *co-cured* and the *cured-on* sandwich coupons are affected by thermal residual strain at room temperature because, in these cases, the layers are integrated at the cure temperature of the composite layers (125 °C). Therefore, a nominal temperature change of ΔT=100 K was considered when the residual strain in the CF/EP layer was estimated. The longitudinal coefficient of thermal expansion (CTE) of the CF/EP and GF/EP composite layers: $\alpha_{CF/EP}$=0.102·10^{-6} [1/K] and $\alpha_{GF/EP}$=5.47·10^{-6} [1/K] were determined using Eq. (4) based on [19].

$$\alpha_{comp} = \frac{V_f\alpha_f E_f + (1 - V_f)\alpha_m E_m}{V_f E_f + (1 - V_f)E_m} \tag{4}$$

Where V_f is the fibre volume fraction (see Table 4), α_f is the CTE of the relevant fibre (see Table 3),

α_m = 6·10^{-5} [1/K] is the CTE of the epoxy matrix estimated from general literature, E_f and E_m are the elastic moduli of the relevant fibre and matrix, respectively. The CTE of the sandwich plate $\alpha_{sandwich} = 2.29$ [1/K] can be estimated similarly using the same formula at a higher structural level as shown in Eq. (5).

$$\alpha_{sandwich} = \frac{V_{CF/EP}\alpha_{CF/EP}E_{CF/EP} + (1 - V_{CF/EP})\alpha_{CF/EP}E_{CF/EP}}{V_{CF/EP}E_{CF/EP} + (1 - V_{CF/EP})E_{GF/EP}} \tag{5}$$

Where $V_{CF/EP}$=0.33 is the volume fraction of the CF/EP layer in the sandwich laminate based on the nominal thicknesses of the layers (1 mm for all three), $E_{CF/EP}$ and $E_{GF/EP}$ are the estimated elastic moduli of the composite layers, respectively (see Table 4). Finally, the thermal residual strain of the CF/EP layer $\varepsilon_{CF/EP}$=-0.022 % can be calculated from the thermal strain of the sandwich plate $\varepsilon_{sandwich}$ and the unconstrained thermal strain of the CF/EP layer $\varepsilon_{CF/EP,\ free}$ using Eq. (6). Negative thermal strain indicating that the CF/EP is under compression at room temperature in the *co-cured* and *cured-on* sandwich coupons was expected, as the CTE of CF/EP is more than 50 times lower than that of the GF/EP material

$$\varepsilon_{CF/EP} = \varepsilon_{sandwich} - \varepsilon_{CF/EP\,free} = (\alpha_{sandwich} - \alpha_{CF/EP})\Delta T \tag{6}$$

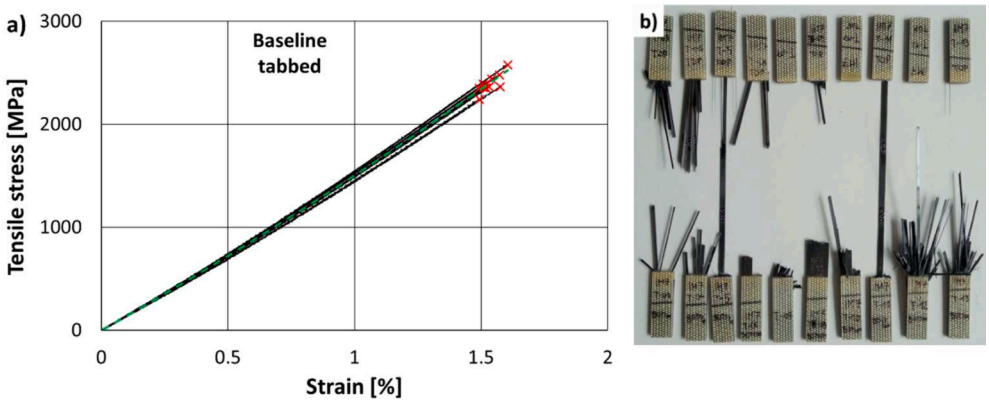

Fig. 5. a) stress–strain curves (with fitted second order polynomial- green dashed line) and b) post-mortem images of the *baseline* coupons.

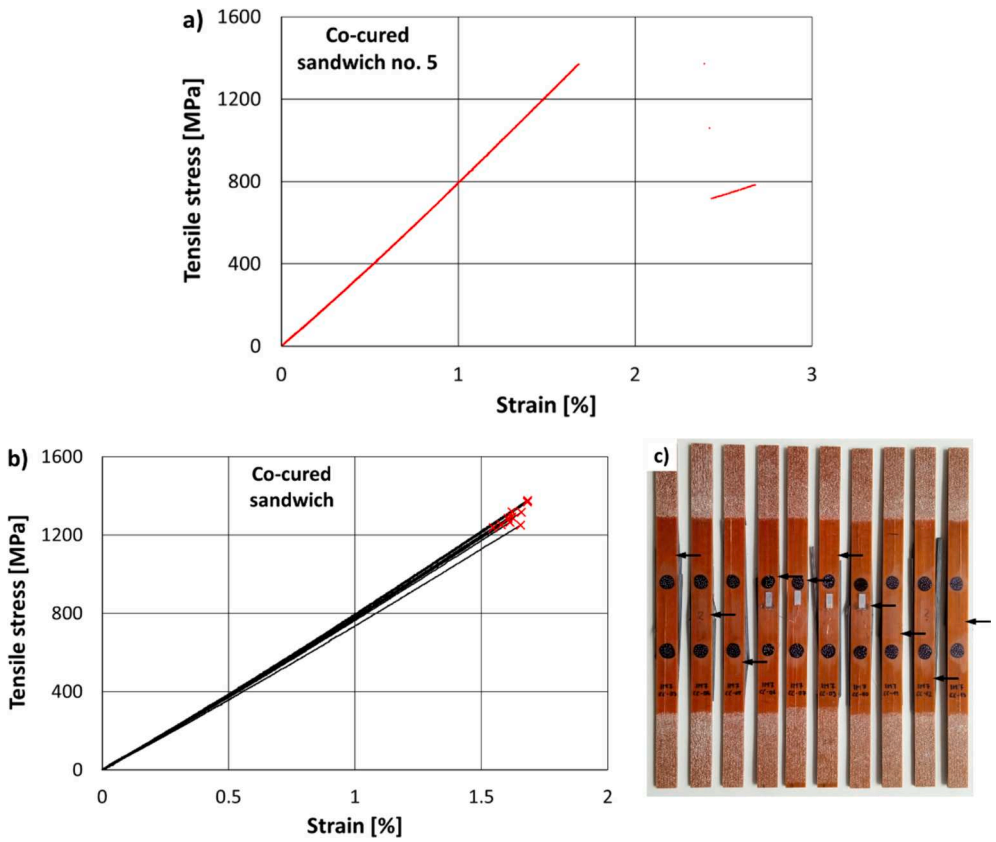

Fig. 6. a) representative full individual stress–strain curve b) stress–strain curves (truncated at CF/EP layer fracture) and c) post-mortem images of the *co-cured* sandwich coupons with arrows showing the CF/EP failure locations.

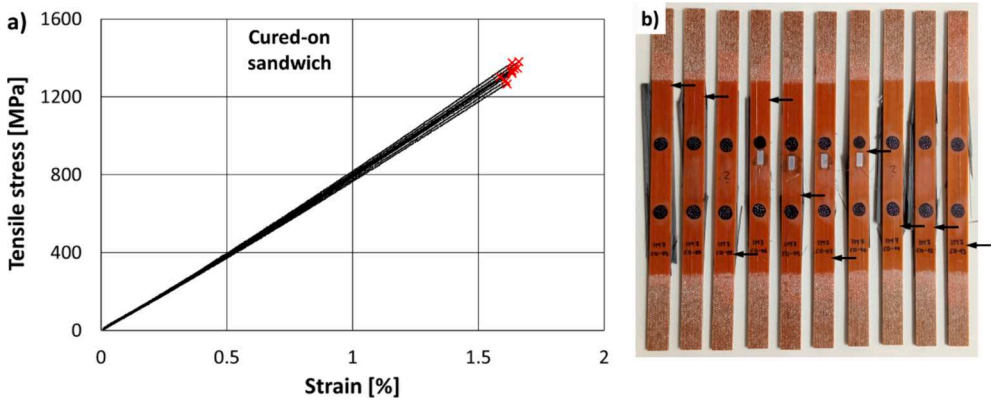

Fig. 7. a) stress–strain curves (truncated at CF/EP layer fracture) and b) post-mortem images of the *cured-on* sandwich coupons with arrows showing the CF/EP failure locations.

4.4. Comparison of the coupon types

Table 6 summarises the tensile test results of the four examined coupon types. The average elastic modulus of the CF/EP material measured with the baseline was slightly higher than the estimated value (141.1 vs 139.3 [GPa] see Table 4). In contrast, the same parameter of the *co-cured* and *cured-on* sandwich coupons was slightly lower than predicted (74.2 and 75.6 vs 77.5 [GPa], see Table 5), but these small deviations are considered acceptable. The *bonded* sandwich coupons had significantly lower average modulus and stress at CF/EP fracture than the other sandwich coupon types due to their thickness being increased by the adhesive layers. Detailed experimental data, including the results at individual coupon level, is provided in Table A1 of the Appendix (section 6).

Fig. 9 compares the failure strain values measured with the four different coupon designs. In case of the *co-cured* and *cured-on* sandwich coupons, the strains are corrected for the thermal effect. Overall, the different coupon series yielded similar results with low scatter. The sandwich coupons showed higher failure strains than the baseline ones, but the difference was not high enough to judge the significance without statistical investigation. Therefore, two-sample Student's t-tests with two-tailed distribution were applied, considering unequal variances (also called Welch-test). The assessment indicated that all three sandwich coupon series resulted in a statistically significant difference in the mean CF/EP failure strains compared to that of the baseline coupon series, but the difference between the CF/EP failure strains obtained with the three different sandwich coupon designs was not statistically significant. The *p*-values obtained from the statistical tests are summarised in Table 7.

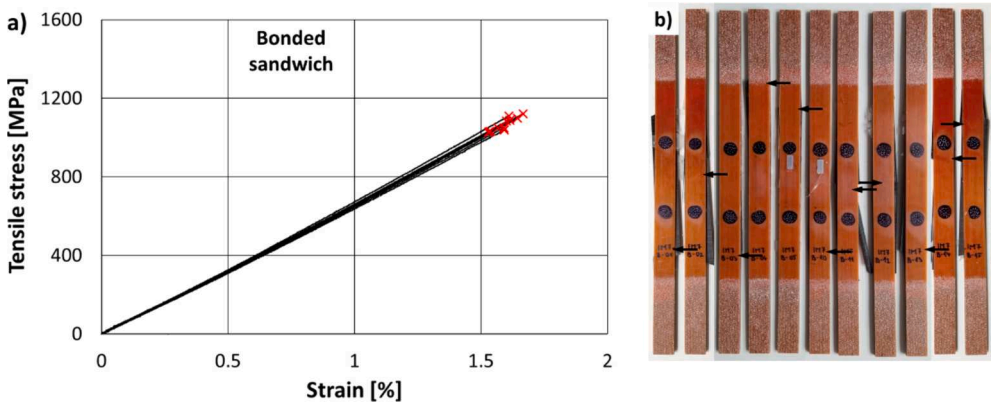

Fig. 8. a) stress–strain curves (truncated at CF/EP layer fracture) and b) post-mortem images of the *bonded* sandwich coupons with arrows showing the CF/EP failure locations.

Table 6
Key average parameters of the tested coupon series (CoV- coefficient of variation in [%]).

Coupon type	Width [mm]	Thickness [mm]	Initial elastic modulus [GPa]	Measured failure strain [%]	Failure stress (coupon) [MPa]	Estimated CF/EP failure stress[a] [MPa]	Thermal corrected failure strain [%]
Baseline tabbed	14.98	0.98	141.1	1.535	2390.7	–	–
CoV	0.2	0.2	2.5	2.5	3.8	–	–
Co-cured sandwich	15.01	2.98	74.2	1.626	1296.3	2561.4	1.605
CoV	0.3	0.3	2.0	2.7	3.8	3.0	2.7
Cured-on sandwich	15.03	2.99	75.6	1.630	1328.1	2567.4	1.608
CoV	0.05	0.7	1.8	1.4	2.8	1.5	1.4
Bonded sandwich	15.03	3.61	62.6	1.589	1065.6	2496.4	–
CoV	0.1	1.2	2.0	2.8	3.3	3.1	–

[a] Calculated by substituting the failure strains in the polynomial of equation (3) fitted to the stress–strain curves of the *baseline* coupons.

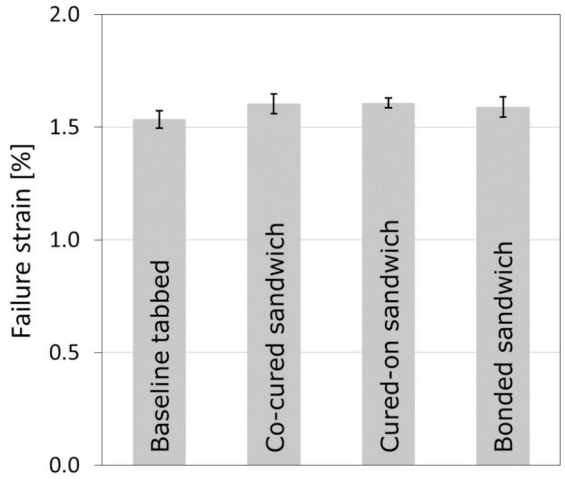

Fig. 9. Comparison of the CF/EP failure strains obtained with the baseline and sandwich coupons.

4.5. Failure mode and position observations

A main advantage of the sandwich coupons is that if they are designed carefully, the GF/EP protective layers can keep the coupon in one piece even after the CF/EP layer fracture since the gripped sections remain bonded. This was exploited in this study for failure location assessment. If the situation was not obvious from the outside, the coupons were opened by inserting a sharp tip object (e.g. screwdriver) between the layers and gently turning it to force the gap open gradually. Fig. 10 shows typical photographs of the opened coupons. It is worth highlighting that in the *co-cured* coupons, a thin but complete layer of the CF/EP remained attached to the GF/EP protective layer, most probably due to the uneven layer interface geometry observed on the micrograph in Fig. 4a. The *cured-on* coupons showed CF/EP residues only locally, while in the *bonded* coupons, no remaining CF/EP was observed on the protective layers (see Fig. 10). The bonded sandwich architecture is therefore considered favourable as it allows full separation of the layers at CF/EP fracture. Interestingly, in most of the opened sandwich coupons, two CF/EP fracture locations were observed: i) one corresponding to the tensile fracture (marked with arrows in Fig. 10) and ii) another one indicating that the dynamic effect of the fracture and unloading of the CF/EP layer at tensile fracture and delamination led to compressive fracture of the layer towards the opposite gripped end of the coupon. This was confirmed by observing typical features like jamming, smashing and fine CF/EP debris at the compressive fracture sites. Please note that since the protective layers remained largely intact after the CF/EP fracture, the broken CF/EP pieces could also have been jammed upon unloading of the sandwich coupon when they were pulled back to the initial length of the coupon.

5. Conclusions

The following conclusions were drawn from the study of different coupon designs to accurately determine the failure strain of unidirectional carbon fibre reinforced epoxy (CF/EP):

- Novel unidirectional sandwich coupons with full-length glass fibre/epoxy (GF/EP) protective layers were developed using three

Table 7
P-values obtained from the Welch-tests of the examined coupon types.

	Baseline	Co-cured	Cured-on	Bonded
Baseline	1			
Co-cured	0.001404	1		
Cured-on	0.000115	0.827859	1	
Bonded	0.007214	0.445245	0.241513	1

Fig. 10. Sandwich coupons opened after CF/EP fracture with arrows showing the CF/EP layer tensile failure locations. The CF/EP layer is attached to the lower part of all three coupons depicted.

different layer integration methods: i) *co-curing* all prepreg plies at once, ii) *curing-on* GF/EP prepreg plies to a solid CF/EP plate iii) *bonding* three cured composite layers together at room temperature. Important indications about the manufacturing difficulties of each coupon design were given, which will help future researchers find an optimal solution for their application.

- Cross-sectional microscopy revealed the transverse undulation of the CF/EP layer in the *co-cured* sandwich coupons, confirmed flat interfaces for the *cured-on* design and consistent bond-line thicknesses for the *bonded* coupon type. *Bonded* sandwich coupons were considered favourable for promoting delamination between the layers at CF/EP fracture and eliminating any unwanted interaction between the layers due to excessive integration.
- A method using a second-order polynomial function fitted to the stress–strain curves of the baseline coupons was presented as a practical means of estimating the tensile strength of the CF/EP material in the sandwich coupons.
- The failure strain values obtained with the sandwich coupon series showed statistically significant increase compared to those obtained with the *baseline tabbed* coupons due to the elimination of stress concentrations near the gripped zones. Whereas the failure strain of the three different sandwich coupon series did not show statistically significant differences.
- The sandwich coupons remained in one piece after the fracture of the CF/EP layer. This unique opportunity was exploited for failure mode and location analysis. A full, thin layer of CF/EP was found on the protective layer of co-cured coupons, indicating too strong connection between the layers, which may influence the failure process of the CF/EP in this coupon type. In case of the bonded coupons, no residual CF/EP was found on the protective layers, confirming full delamination.
- The *bonded* sandwich coupons were found outstanding as they ensured flat layer interfaces, full delamination between the layers upon CF/EP failure and did not require thermal residual strain correction. Therefore, this coupon type is recommended for further development.

CRediT authorship contribution statement

Gergely Czél: Writing – original draft, Visualization, Supervision, Resources, Methodology, Investigation, Funding acquisition, Conceptualization.

Declaration of competing interest

The authors declare that they have no known competing financial interests or personal relationships that could have appeared to influence the work reported in this paper.

Data availability

No data was used for the research described in the article.

Acknowledgement

The research was supported by the National Research, Development and Innovation Office (NRDI, Hungary) through grant OTKA FK 131882, and by the Ministry of Culture and Innovation of Hungary from the National Research, Development and Innovation Fund, under the TKP2021-NVA funding scheme through grant no. TKP-6-6/PALY-2021 and from the Complex Development funding scheme through grant no. 2022-2.1.1-NL-2022-00012 Creation of National Laboratories. The author is grateful for support through the János Bolyai Research Scholarship of the Hungarian Academy of Sciences and the ÚNKP-23-5-BME-433 New National Excellence Program of the Ministry of Culture and Innovation of Hungary allocated from the source of the National Research, Development and Innovation Fund. Special thanks to András Jandrics for his help with the experiments.

6. Appendix

6.1. Tabbing of the baseline coupons

The 300x300 mm cured test plate was prepared for bonding of the end-tabs. The bonding areas were lightly abraded with rough sandpaper to increase the bonding area and then degreased with methanol. 300x50 mm plates of glass/epoxy tab material were prepared the same way and secured in place with masking tape pieces in a way that the tab plates could be folded back to allow the application of the adhesive with a spatula. The CF/EP

test plate with the end tab pieces was kept flat between glass plates and under sufficient mass (to squeeze out the excess adhesive) for 24 h at room temperature until the epoxy adhesive was fully cured.

6.2. Lay-up of co-cured sandwich plates

Four-ply monolithic CF/EP and GF/EP blocks were prepared and debulked under vacuum first, and then they were joined into a three-layer UD sandwich plate and debulked again for min. 10 min. Special care was taken to maintain the same fibre orientation in all layers when stacking them together, as it was key across all manufacturing steps to maintain a precise reference edge for future cutting of the test coupons. This was a key priority in the manufacturing of all sandwich plates. The sandwich plate was cured the same way as the baseline one using the thick top plate and sufficiently high silicone dam around the laminate in the vacuum bag to ensure uniform thickness.

6.3. Developed procedure for bonding three 300x300 mm UD composite plates to make a sandwich plate

6.3.1. Positioning the plates

One edge of each plate was maintained as a reference for fibre orientation throughout the lay-up and curing processes. These reference edges were used to assemble the sandwich plate with parallel fibre directions in all layers. Two opposite corners of the stack were selected, and approx. 20x20 mm pieces of double-sided adhesive tape were used to secure all the plates in the preferred position. Then, 8 mm holes were drilled with a pillar drill and a simple diamond particle coated tool (originally designed for wet drilling of glass plates) to the corners where the adhesive tapes were inserted between the layers. The adhesive tapes helped keeping the plates tightly together and minimised dust/slurry penetration between them, thereby improved the quality of the holes significantly. After marking the positions, the plates were separated, the double-sided adhesive tape pieces were removed, the bonding surfaces were lightly abraded with rough sandpaper and were degreased with methanol. 8 mm diameter 3D printed buttons were prepared to position the plates while the adhesive was curing (see fig. A1a). Suitable dimensions were selected after careful consideration: the height was set just below the expected thickness of the sandwich plate, and the diameter to fit loosely in the drilled holes. This was important to make sure that the buttons did not hold the flat compression plates up (resulting in uneven thickness) and did not let the three plates displace during the adhesive curing stage (compromising parallel fibre directions in all layers). Both scenarios could easily render the sandwich plate unsuitable for tensile testing the CF/EP layer in the middle.

6.3.2. Application and spreading of the adhesive

After a number of attempts, the stripy pattern shown in fig. A1b was found optimal as the channels formed by the adhesive paste let the air escape if compression force is applied gradually and slowly from one edge, e.g. through a heavy roller (see fig. A1c). In response to the compression force gradually applied on the adherend plates, the adhesive paste spreads, and the vetted areas gradually join up without trapping air. It is recommended to apply the adhesive stripes with equal spacing and in an amount designed in advance to ensure a consistent bond-line thickness over the whole bonding area. The stripes can be made with a spatula (as in fig. A1b) or with a dosing gun and a static mixer head. It is useful to apply the stripes perpendicular to the fibre direction in the UD adherend plates as they are more compliant in this direction, which makes it easier to keep a gap at the far end initially and bend the plates with the roller to spread the adhesive. The spacer should be removed after the roller passed over about half of the plate. It is recommended that all three layers be bonded together in one operation (possibly with two batches of adhesive mixed separately) to avoid any inconsistencies due to slightly different cure conditions. It is convenient to insert the positioning buttons in the holes after bonding the first two plates and secure them with adhesive tapes to stop any unwanted slippage of the plates during the bonding of the third plate to the stack.

6.3.3. Curing the adhesive

A key feature of the bonded sandwich coupons is that they do not suffer from unwanted residual stresses due to the different CTE values of the plates. For this, the bonding has to take place at room temperature. Therefore, no external heat was applied to the sandwich plates. Sufficient pressure must be applied to ensure uniform adhesive layer thickness. The simplest way is to put the stack between stiff, flat plates and apply force by weight precisely positioned in the middle of the stack. This simple method was selected as vacuum consolidation was apparently not uniform enough (possibly due to bag stretching along the edges of the top plate on the bonded sandwich), and the required pressure was not high, so there was no need to use a hydraulic press. A stack of an 8 mm Al base plate, the sandwich plate between release films, a 20 mm thick steel plate and additional steel cylinders to apply extra force was built. In total, up to 400 N force was applied through a thick steel plate, which was judged sufficient as a significant amount of excess adhesive was squeezed out from both bonding areas. The loose fit of the positioning buttons was confirmed before the stack was built. The sandwich plate was left to cure under load at room temperature for a minimum of 24 h.

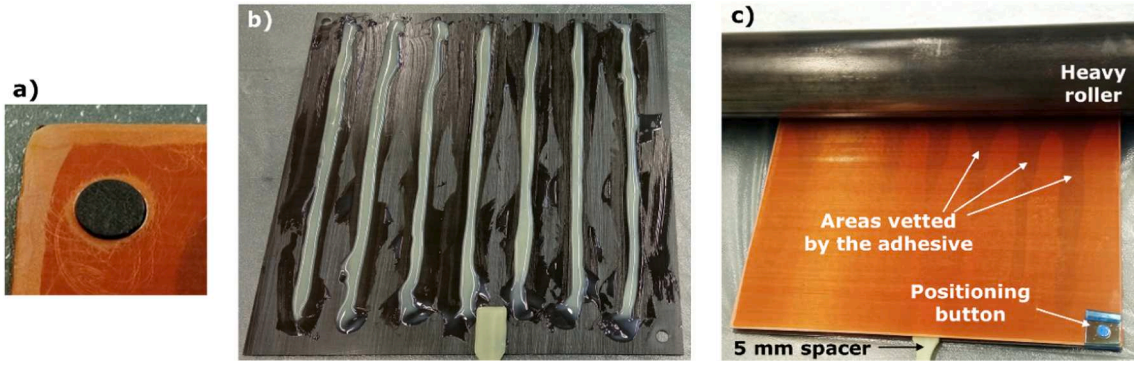

Fig. A1. Key features of the developed sandwich plate bonding methodology: a) 8 mm diameter positioning button, b) adhesive applied manually in a stripy pattern, c) spreading the adhesive using a heavy roller and opening gap

Table A1
Detailed test data of the four examined coupon types (CoV- coefficient of variation in [%]).

Coupon type	Coupon no.	Width [mm]	Thickness [mm]	Initial elastic modulus [Gpa]	Failure strain [%]	Failure stress (coupon) [MPa]	Estimated CF/EP failure stress [MPa]	Thermal corrected failure strain [%]
Baseline tabbed	1	14.97	0.976	139.4	1.518	2352.2	–	–
	2	14.93	0.978	142.6	1.604	2576.8	–	–
	3	15.04	0.979	143.8	1.573	2477.5	–	–
	4	15.01	0.980	143.8	1.542	2438.4	–	–
	5	14.91	0.983	135.3	1.576	2362.5	–	–
	6	14.97	0.982	136.4	1.493	2241.8	–	–
	7	14.99	0.980	143.5	1.492	2347.6	–	–
	8	15.00	0.981	141.8	1.511	2356.0	–	–
	9	14.99	0.983	145.9	1.508	2391.6	–	–
	10	14.96	0.983	138.8	1.532	2363.1	–	–
	Average	14.98	0.980	141.1	1.535	2390.7	–	–
	St.Dev.	0.036	0.002	3.507	0.038	89.88	–	–
	CoV	0.239	0.240	2.49	2.49	3.76	–	–
Co-cured sandwich	1	14.89	2.966	75.00	1.684	1376.9	2663.0	1.662
	2	15.05	2.972	74.35	1.580	1253.1	2479.3	1.558
	3	15.04	2.978	75.47	1.682	1369.6	2659.4	1.660
	4	15.04	2.980	74.76	1.547	1237.5	2421.7	1.525
	5	15.03	2.985	70.35	1.655	1249.7	2612.4	1.633
	6	15.04	2.984	73.12	1.612	1264.7	2536.5	1.590
	7	15.04	2.981	74.65	1.605	1285.9	2524.4	1.584
	8	15.00	2.977	73.94	1.620	1292.0	2549.1	1.598
	9	15.00	2.968	75.29	1.621	1318.2	2552.5	1.600
	10	14.97	2.959	74.65	1.657	1315.6	2616.0	1.636
	Average	15.01	2.975	74.16	1.626	1296.3	2561.4	1.605
	St.Dev.	0.050	0.008	1.50	0.044	48.69	77.44	0.04
	CoV	0.332	0.283	2.02	2.70	3.76	3.02	2.74
Cured-on sandwich	1	15.03	2.965	74.29	1.609	1282.3	2531.2	1.587
	2	15.03	2.981	77.35	1.661	1380.0	2622.7	1.639
	3	15.02	2.996	75.94	1.643	1344.7	2590.2	1.621
	4	15.02	3.003	73.24	1.614	1265.7	2539.2	1.592
	5	15.04	3.009	75.94	1.635	1320.5	2575.7	1.613
	6	15.03	3.013	75.53	1.655	1347.9	2611.4	1.633
	7	15.02	3.005	76.24	1.586	1301.8	2489.9	1.564
	8	15.03	2.993	75.41	1.633	1335.7	2572.7	1.611
	9	15.02	2.977	74.53	1.629	1327.4	2566.6	1.608
	10	15.02	2.956	77.76	1.634	1374.7	2574.0	1.612
	Average	15.03	2.990	75.62	1.630	1328.1	2567.4	1.608
	St.Dev.	0.007	0.019	1.37	0.022	37.03	39.12	0.022
	CoV	0.045	0.651	1.81	1.36	2.79	1.52	1.38
Bonded sandwich	1	15.04	3.580	62.47	1.644	1098.1	2593.1	–
	2	15.03	3.608	62.35	1.590	1049.2	2497.7	–
	3	15.03	3.638	63.29	1.537	1031.0	2405.3	–
	4	15.04	3.651	61.53	1.591	1037.9	2499.4	–
	5	15.03	3.657	63.59	1.615	1088.4	2540.5	–
	6	15.04	3.606	62.94	1.530	1025.1	2393.0	–
	7	15.04	3.587	63.35	1.600	1083.4	2515.4	–
	8	14.99	3.584	64.65	1.610	1109.2	2531.8	–
	9	15.03	3.573	62.82	1.567	1048.7	2457.1	–
	10	15.02	3.558	63.06	1.532	1029.5	2395.6	–
	11	15.02	3.539	63.06	1.666	1120.6	2631.4	–
	Average	15.03	3.60	63.01	1.589	1065.6	2496.4	–
	St.Dev.	0.013	0.038	0.786	0.045	35.04	78.63	–
	CoV	0.089	1.05	1.25	2.82	3.29	3.15	–

References

[1] ASTM D3039/D3039M Standard Test Method for Tensile Properties of Polymer Matrix Composite Materials.

[2] ISO 527-5 Plastics - Determination of tensile properties - Part 5: Test conditions for unidirectional fibre-reinforced plastic composites.

[3] Wisnom MR, Atkinson JW. Reduction in tensile and flexural strength of unidirectional glass fibre-epoxy with increasing specimen size. Comp Struct 1997; 38:405–11. https://doi.org/10.1016/S0263-8223(97)00075-5.

[4] Wisnom MR, Khan B, Hallett SR. Size effects in unnotched tensile strength of unidirectional and quasi-isotropic carbon/epoxy composites. Comp Struct 2008;84: 21–8. https://doi.org/10.1016/j.compstruct.2007.06.002.

[5] Hojo M, Sawada Y, Miyairi H. Influence of clamping method on tensile properties of unidirectional CFRP in 0 ∘ and 90 ∘ directions- round robin activity for international standardization in Japan. Composites 1994;25:786–96.

[6] De Baere I, Van Paepegem W, Degrieck J. On the design of end tabs for Quasi-static and fatigue testing of fibre-reinforced composites. Polym Compos 2009;30:381–90. https://doi.org/10.1002/pc.20564.

[7] Kulakov VL, Tarnopol'skii YM, Arnautov AK, Rytter J. Stress-strain state in the zone of load transfer in a composite specimen under uniaxial tension. Mech Compos Mater 2004;40:91–100. https://doi.org/10.1023/B:MOCM.0000025483.37317.e2.

[8] Korkiakoski S, Brøndsted P, Sarlin E, Saarela O. Influence of specimen type and reinforcement on measured tension-tension fatigue life of unidirectional GFRP laminates. Int J Fatigue 2016;85:114–29. https://doi.org/10.1016/j.ijfatigue.2015.12.008.

[9] Kumar R, Mikkelsen LP, Lilholt H, Madsen B. Experimental method for tensile testing of unidirectional carbon fibre composites using improved specimen type and data analysis. Materials 2021;14:393–9. https://doi.org/10.3390/ma14143939.

[10] Czél G, Wisnom MR. Demonstration of pseudo-ductility in high performance glass-epoxy composites by hybridisation with thin-ply carbon prepregs. Compos A Appl Sci Manuf 2013;52:23–30. https://doi.org/10.1016/j.compositesa.2013.04.006.
[11] Czél G, Jalalvand M, Wisnom MR. Design and characterisation of advanced pseudo-ductile unidirectional thin-ply carbon/epoxy-glass/epoxy hybrid composites. Compos Struct 2016;143:362–70. https://doi.org/10.1016/j.compstruct.2016.02.010.
[12] Czél G, Jalalvand M, Wisnom MR. Hybrid specimens eliminating stress concentrations in tensile and compressive testing of unidirectional composites. Compos Part A Appl Sci Manuf 2016;91:436–47. https://doi.org/10.1016/j.compositesa.2016.07.021.
[13] Adams DO, Adams DF. Tabbing Guide for Composite Test Specimens. Technical report, Office of Aviation Research: Washingthon D.C; 2002. https://apps.dtic.mil/sti/pdfs/ADA411472.pdf.
[14] Portnov GG, Kulakov VL, Arnautov AK. A refined stress-strain analysis in the load transfer zone of flat specimens of high-strength unidirectional composites in uniaxial tension 2. Finite-element parametric analysis Mech Compos Mater 2007;43:29–40. https://doi.org/10.1007/s11029-007-0003-5.
[15] Fazlali B, Upadhyay S, Ashodia SA, Mesquita F, Lomov SV, Carvelli V, et al. Specimen designs for accurate tensile testing of unidirectional composite laminates. Compos A Appl Sci Manuf 2023;175:107799. https://doi.org/10.1016/j.compositesa.2023.107799.
[16] Fazlali B, Lomov SV, Swolfs Y. Concerns in tension-tension fatigue testing of unidirectional composites: Specimen design and test setup. Compos B Eng 2024;272:111213. https://doi.org/10.1016/j.compositesb.2024.111213.
[17] Marino SG, Czél G. Improving the performance of pseudo-ductile hybrid composites by film-interleaving. Compos A Appl Sci Manuf 2021;142:106233. https://doi.org/10.1016/j.compositesa.2020.106233.
[18] Czél G, Jalalvand M, Wisnom MR, Czigány T. Design and characterisation of high performance, pseudo-ductile all-carbon/epoxy unidirectional hybrid composites. Compos B Eng 2017;111:348–56. https://doi.org/10.1016/j.compositesb.2016.11.049.
[19] Schapery RA. Thermal expansion coefficients of composite materials based on energy principles. J Compos Mater 1968;2:380–404. https://doi.org/10.1177/002199836800200308.